



Since January 2020 Elsevier has created a COVID-19 resource centre with free information in English and Mandarin on the novel coronavirus COVID-19. The COVID-19 resource centre is hosted on Elsevier Connect, the company's public news and information website.

Elsevier hereby grants permission to make all its COVID-19-related research that is available on the COVID-19 resource centre - including this research content - immediately available in PubMed Central and other publicly funded repositories, such as the WHO COVID database with rights for unrestricted research re-use and analyses in any form or by any means with acknowledgement of the original source. These permissions are granted for free by Elsevier for as long as the COVID-19 resource centre remains active.



Imaging of Multisystem Inflammatory Disease in Children (MIS-C) Associated With COVID-19

Figen Palabiyik, Nihal Akcay, Esra Sevketoglu, Nevin Hatipoglu, Emine Ergul Sari, Ercan Inci

Rationale and Objectives: To retrospectively evaluate imaging findings in multisystem inflammatory disease in children associated with COVID-19 (MIS-C).

Materials and Methods: The radiological imaging findings of 45 pediatric patients aged between 52 days and 16 years, who were diagnosed with MIS-C according to the World Health Organization (WHO) criteria, were evaluated. All the patients underwent chest X-ray and echocardiography. The findings obtained from 25 abdominal radiographs, 24 abdominal US, 7 abdominal CT, 16 thorax CT, 21 cranial MRI and one spinal MRI, MR cholangiography (MRCP) and cardiac MRI examinations were categorized and evaluated according to the affected systems.

Results: While the most common findings in chest X-ray were perihilar opacity and peribronchial thickening, pleural effusion was the most finding in thorax CT. Echocardiography findings of myocarditis were observed in 31% of the cases. The most common findings in abdominal radiological evaluation were hepatomegaly and splenomegaly, edema in the gallbladder wall and periportal area, mesenteric lymph nodes in the right lower quadrant, thickening of the intestinal walls, and free fluid. Reversible splenic lesion syndrome (RESLES) was the most common neurological finding. Acute disseminated encephalomyelitis (ADEM)-like lesions, acute hemorrhagic necrotizing encephalomyelitis, and radiological findings consistent with Guillain-Barré syndrome were found in one case each.

Conclusion: Radiological findings seen in MIS-C in pediatric cases are correlated with the affected system. According to the system involved, there is no specific finding for this disease. Radiological findings are not the primary diagnostic tool but can assist in the evaluation of the affected systems and to guide treatment.

Key Words: Children; COVID-19; Imaging; Multisystem inflammatory syndrome in children; Radiology.

© 2021 The Association of University Radiologists. Published by Elsevier Inc. All rights reserved.

INTRODUCTION

When the coronavirus disease 2019 (COVID-19) infection first occurred, it was shown that children survived this infection less often than adults in the acute disease. However, in the later stages of the pandemic, symptoms similar to severe multisystemic hyperinflammatory syndrome that did not resemble the acute form of COVID-19 began to be observed in children. Multisystem

inflammatory syndrome in children associated with COVID-19 (MIS-C) was reported for the first time in April 2020 in children from the UK and the USA, who were previously healthy but were determined to have a positive severe acute respiratory syndrome coronavirus 2 (SARS-CoV-2) reverse transcription-polymerase chain reaction (RT-PCR) or serology testing for SARS-CoV-2. Fever, abdominal pain, rash and conjunctivitis, and increased acute phase reactants and cardiac markers, often accompanied by hypotensive shock and myocardial dysfunction have been identified in children diagnosed with MIS-C. In MIS-C, there is a previous COVID-19 infection in children, a family history of the disease, or a history of contact with an infected individual, and symptoms occur approximately within two to three weeks after COVID-19. Unlike acute COVID-19 infection, many systems are affected due to the inflammatory response that develops, and some radiological findings occur due to the pathologies that occur. Although radiological findings are not typical, they may be of warning findings for the diagnosis of MIS-C when correlated with clinical and laboratory findings and if other pathologies are excluded.

Acad Radiol 2021; 28:1200–1208

From the University of Health Sciences, Bakirkoy Dr. Sadi Konuk Training and Research Hospital, Department of Pediatric Radiology, Istanbul, Turkey (F.P.); University of Health Sciences, Bakirkoy Dr. Sadi Konuk Training and Research Hospital, Department of Pediatric Intensive Care, Istanbul, Turkey (N.A., E.S.); University of Health Sciences, Bakirkoy Dr. Sadi Konuk Training and Research Hospital, Department of Pediatric Infection, Istanbul, Turkey (N.H.); University of Health Sciences, Bakirkoy Dr. Sadi Konuk Training and Research Hospital, Department of Pediatric Diseases, Istanbul, Turkey (E.E.S.); University of Health Sciences, Bakirkoy Dr. Sadi Konuk Training and Research Hospital, Department of Radiology, Istanbul, Turkey (E.I.). Received April 14, 2021; revised May 24, 2021; accepted May 24, 2021. **Address correspondence to:** F.P. e-mail: figen_dr@yahoo.com

© 2021 The Association of University Radiologists. Published by Elsevier Inc. All rights reserved.

<https://doi.org/10.1016/j.acra.2021.05.030>

There are few publications on the radiological imaging of MIS-C in the literature, but they report non-specific radiological findings. Sharing radiological findings from different countries on this subject will increase knowledge and awareness. The aim of this study was to retrospectively report the radiological findings of children diagnosed with MIS-C as a result of various system involvement in our pandemic hospital.

MATERIALS AND METHODS

Patient selection criteria

Forty-five pediatric patients who presented to the pediatric department of our hospital between March 2020 and March 2021 and were diagnosed with MIS-C were retrospectively evaluated. The clinical and laboratory findings and chest X-ray, echocardiography, abdominal radiography, ultrasonography (US), computed tomography (CT) and magnetic resonance imaging (MRI) images of all cases were evaluated. Written consent was provided by the parents of the cases after obtaining approval from the ethics committee of our hospital.

Diagnostic criteria for MIS-C associated with COVID-19

The patients were diagnosed with MIS-C according to the WHO criteria for MIS-C (Table 1). All cases underwent the RT-PCR testing of the upper respiratory tract and serology for SARS-CoV-2 antibodies using blood or cerebrospinal fluid (CSF) samples. The history of COVID-19 in the family was investigated by determining whether the cases had previously tested positive for the disease or had a history of contact

TABLE 1. Case Definitions for MIS-C (Obtained From WHO)

Children and adolescents aged 0–19 years with fever ≥ 3 days AND two of the following:

1. Rash or bilateral non-purulent conjunctivitis or mucocutaneous inflammation signs (oral, hands or feet)
2. Hypotension or shock
3. Features of myocardial dysfunction pericarditis, valvulitis or coronary abnormalities (including echocardiographic findings or elevated troponin/NT-proBNP)
4. Evidence of coagulopathy (based on PT, PTT, and elevated D-dimer levels)
5. Acute gastrointestinal problems (diarrhea, vomiting or abdominal pain)

AND

Elevated markers of inflammation, such as ESR, CRP and procalcitonin

AND

No other obvious microbial cause of inflammation, including bacterial sepsis, staphylococcal or streptococcal shock syndromes

AND

Evidence of COVID-19 (RT-PCR assay, antigen test or serology positivity) or possible contact with a patient with COVID-19

Consider this syndrome in children with features of typical or atypical Kawasaki disease or toxic shock syndrome.

with an infected individual. Only cases with RT-PCR and serology positivity according to the WHO criteria were accepted as MIS-C and included in the study.

Image analysis

The picture archiving and communication system (PACS) of hospital was scanned to review all imaging studies performed on children with MIS-C associated with COVID-19. Chest and abdominal radiography, echocardiography, abdominal US, thorax and abdominal CT, cranial and spinal MRI, MR angiography, MRCP, and cardiac MRI examinations were evaluated by a pediatric radiologist with 11 years of experience.

Chest X-ray and thorax CT were evaluated in terms of interstitial and alveolar opacities, distribution (unilateral or bilateral, central or peripheral), zonal distribution (upper, middle or lower zone) and focality (single, multifocal or diffuse). While parenchymal pathologies were examined in terms of peribronchial thickening, ground glass appearance, consolidation, atelectasis and pulmonary edema, the presence of pleural effusion, mediastinal and hilar lymphadenopathy, and pulmonary embolism was also investigated. Heart size, right and left ventricular function, and pericardial effusion were evaluated using echocardiography.

Abdominal radiographs were evaluated in terms of ileus and obstruction, and enlargement in the intestinal loops and wall thickening. In abdominal US and abdominal CT, liver, spleen and kidney dimensions, parenchymal anomalies observed in solid organs (echogenicity and density differences and heterogeneity), periportal edema in the liver and pericholecystic wall edema were evaluated. In addition, the presence of distension, wall thickness in visceral organs (gall bladder, stomach, bowel loops, and bladder) was investigated. If the wall thickness was over 3 mm, it was considered as thickening. Intraabdominal free fluid and abdominal lymphadenopathy were explored. The lymph nodes were considered enlarged if they were over 5 mm in the short axis.

Cranial MRI was used to reveal pathological signal changes and distributions observed in cerebral and cerebellar parenchyma and brainstem, distribution of lesions, and areas of involvement (deep white matter, subcortical white matter, cortex, and basal ganglion), and contrast enhancement of lesions, diffusion characteristics, thrombus and infarction, and bleeding. In MR angiography, venous structures were evaluated in terms of thrombus, arterial structures in terms of thrombus, and aneurysmal dilatation.

RESULTS

Of the 45 child cases, 27 were boys (60%) and 18 were girls (40%), aged 52 days to 16 years, with a median age of 7.68 years. Six cases (13%) had a history of previous COVID-19 disease 2–3 weeks ago and 18 (40%) had a family history of COVID-19. In other cases (46%), previous COVID-19 infection, family history of COVID-19, and history of contact with an infected individual

were not detected. RT-PCR and serology positivity was detected in two patients (4%) while PCR was negative in 43 cases (96%) with a positive serology test. CSF serology was evaluated as positive in two cases. One patient with severe multisystem involvement and three with neurological involvement were discharged from the hospital with neurological sequelae. More than one system involvement was observed in all patients admitted to the intensive care unit (69%) and in three patients (7%) hospitalized in the pediatric service. Thirty-one patients (69%) were followed up in the intensive care unit, and 14 (31%) in the pediatric service. None of the patients had a history of chronic disease. Mortality was not observed. Eight patients (17.7%) were intubated.

The most frequently reported general and gastrointestinal symptoms were fever and vomiting, abdominal pain, and diarrhea, rash, conjunctivitis and weakness. Respiratory symptoms were cough and respiratory distress while neurological symptoms included seizure, neck stiffness, and inability to walk (Table 2). In all cases, the white blood cell count, C-reactive protein (CRP), ferritin, D-dimer, troponin and fibrinogen values were high, and the albumin values were low. The amylase and lipase levels were found to be high in seven cases. Ventricular dysfunction and signs of myocarditis were detected in 14 cases. The clinical, laboratory and radiological findings of the patients with a diagnosis of MIS-C are summarized in Tables 2 and 3.

Thorax

Chest X-ray was performed in all cases. No lung findings were observed in 35 cases (78%). The most common findings were perihilar opacity and peribronchial thickening seen in

TABLE 2. The Clinical and Laboratory Findings in Children for MIS-C

Children (n = 45)	N (%)
COVID-19 testing	
RT-PCR-/serology+	43 (96%)
BOS serology+	2 (5%)
RT-PCR+/serology+	2 (4%)
Sign and symptoms	
General	
Fever	42 (93%)
Weakness	40 (89%)
Rash	15 (33%)
Conjunctivitis	3 (7%)
Thorax	
Cough	9 (20%)
Respiratory distress	9 (20%)
Cardiac	
Myocardial dysfunction	14 (31%)
Abdomen	
Abdominal pain	28 (62%)
Vomiting	20 (44%)
Central nervous system	
Seizure	14 (31%)
Neck stiffness	6 (13%)
Inability to walk	1 (2%)

TABLE 3. Imaging Findings in Patients With MIS-C

Children (n = 45)	n(%)
Imaging	
Chest X-ray	45 (100%)
Thorax CT	16 (36%)
Echocardiography	45 (100%)
Cardiac MRI	1 (2%)
Abdominal X-ray	25 (56%)
Abdominal US	24 (53%)
Abdominal CT	7 (16%)
MRCP	1 (2%)
Cranial MRI	21 (47%)
Spinal MRI	2 (4%)
Thorax	
No findings	35 (78%)
Perihilar opacity and peribronchial thickening	9 (20%)
Atelectasis and consolidation	4 (9%)
Pleural effusion	5 (11%)
Diffuse ground glass appearance	1 (2%)
Cardiac	
No finding	31 (69%)
Decrease in systolic function	14 (31%)
Pericardial effusion	1 (2%)
Abdomen	
Hepatomegaly	7 (16%)
Hepatosplenomegaly	2 (4%)
Periportal and pericholecystic edema	3 (7%)
Multiple mesenteric lymph nodes	6 (13%)
Free fluid	5 (11%)
Temporary invagination	1 (2%)
Echogenic kidneys	1 (2%)
Intestinal wall thickening	5 (11%)
Pancreatitis	1 (2%)
Cholestasis	1 (2%)
Thrombus in the inferior vena cava	1 (2%)
Central nervous system	
No finding	4 (9%)
RESLES	6 (13%)
ADEM-like lesions	1 (2%)
PRES	1 (2%)
Acute hemorrhagic necrotizing encephalomyelitis	1 (2%)
Cerebral and cerebellar atrophy	1 (2%)
Guillain-Barré syndrome	1 (2%)

chest X-ray (Fig 1a). The most common finding on thorax CT was pleural effusion (Fig 1b). Diffuse lung opacity in chest X-ray and diffuse ground glass appearance and consolidation in thorax CT were observed in one patient (Fig 1c, d).

Cardiac

Echocardiography was performed in all cases diagnosed with MIS-C. Echocardiography was normal in 31 cases (31%), varying degrees of decrease in systolic functions and ejection fraction consistent with myocarditis were detected. In the severe case with multiple system involvement, dilated

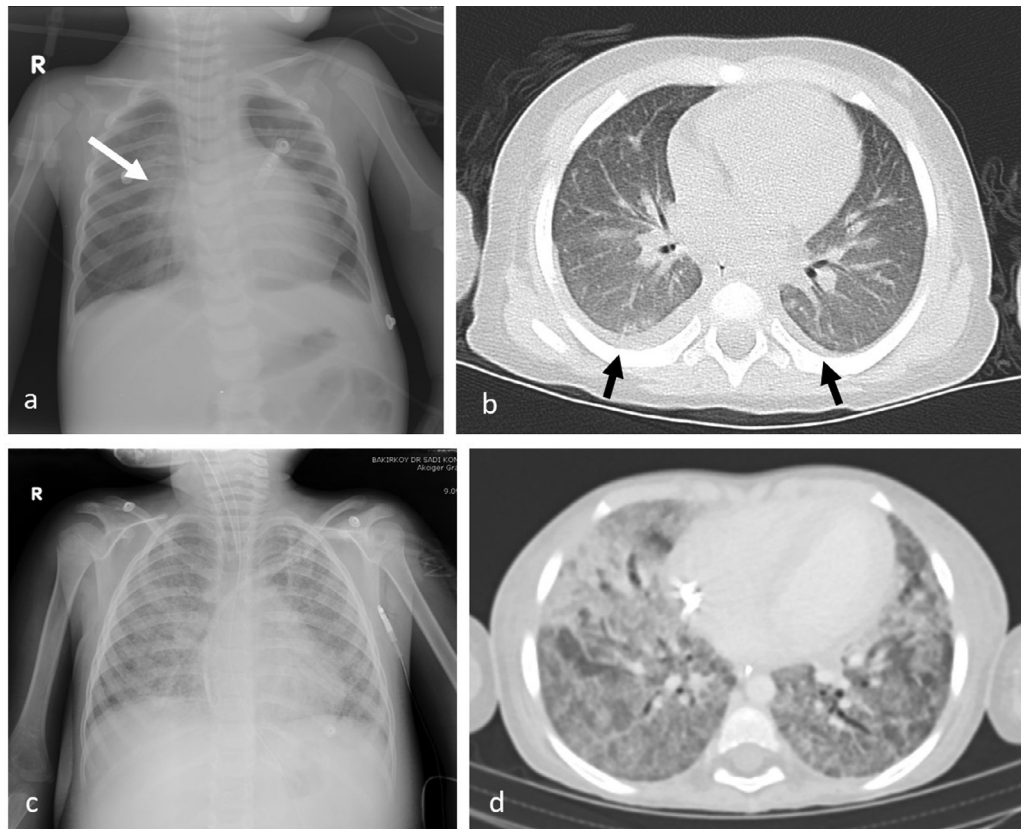


Fig 1. Chest X-ray of a 24-month-old male with perihilar opacity and peribronchial thickening (white arrow) (a). Thorax CT examination of a 23-month-old female showing bilateral pleural effusion (black arrows) (b). Chest X-ray and thorax CT of a four-year-old female with increased bilateral diffuse opacity, diffuse ground glass density, and consolidation (c, d).

cardiomyopathy was observed along with myocarditis and pericardial effusion findings. Cardiac MRI showed a marked decrease in pericardial effusion and systolic functions and an increase in cardiac dimensions.

Abdomen

The most common finding on abdominal radiography was air-fluid level observed in four cases. The most common US findings were hepatomegaly and hepatosplenomegaly. Periportal and pericholecystic wall edema, multiple mesenteric lymph nodes in the right lower quadrant, free fluid in the abdomen, temporary invagination, and echogenic kidneys were seen (Fig 2a–c). Abdominal CT was performed in five cases that could not be clinically distinguished from acute appendicitis. While the appendix was evaluated as normal in these cases, periportal and pericholecystic wall edema, thickening of the intestinal walls, presence of free fluid in the abdomen, multiple lymph nodes in the right lower quadrant, and prominence of mesenteric vascular structures were observed. Appendicitis could not be clearly differentiated with this ultrasound these patients. All other abdominal findings observed were similar to ultrasound findings. In a severe case, the CT examination was undertaken following the detection of an increase in the amylase and lipase values,

heterogeneity in the pancreas, and multiple hypoechoic areas in the parenchyma. During the treatment, amylase and lipase levels of the patients increased for the second time. The repeated abdominal CT examination revealed that the pancreatic dimensions decreased and the hypodense areas observed in the pancreatic parenchyma turned into necrotic areas (Fig 2d). In the same case, intrahepatic bile ducts and pancreatic canal were found to be enlarged in abdominal US and MRCP (Fig 2e, f) due to cholestasis that developed during treatment. In one case, a thrombus was observed in the inferior vena cava.

Central nervous system

Various cranial neurological findings (headache, epilepsy, hallucination, neck stiffness, and inability to walk) were observed in the clinical examination of 14 cases (31%). The most common cranial MRI finding was RESLES. In six of these cases, diffusion restriction was detected in the posterior part of the splenium in diffusion-weighted MRI sequences (Fig 3). The patients' complaints resolved with the initiation of treatment, and the control diffusion MRI examination indicated that the lesion had completely disappeared. In one patient who presented with hallucinations and seizures, cranial MRI showed symmetrical signal changes in the cerebellar

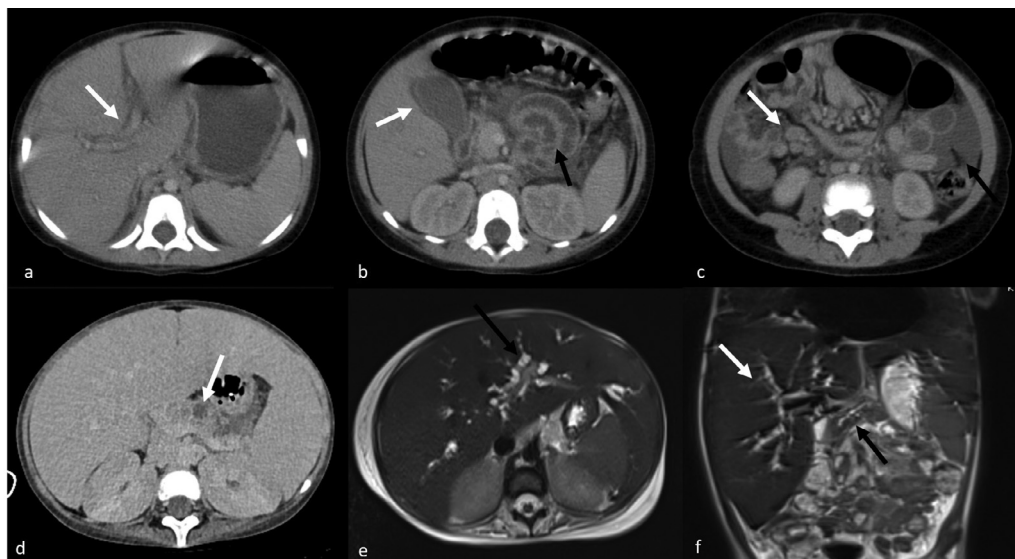


Fig 2. Abdominal CT images of a 23-month-old female showing, periportal edema (white arrow) (a), edema around the gallbladder (white arrow), thickening of the intestinal walls (black arrow) (b), multiple lymph nodes in the right lower quadrant (white arrow), and free fluid (black arrow) (c). Abdominal CT image of a four-year-old female showing decreased dimension, heterogeneity in the pancreas, and necrotic areas in the parenchyma (white arrow) (d). MRCP showing the enlargement of intrahepatic bile ducts and main pancreatic duct in the same child (e, f).

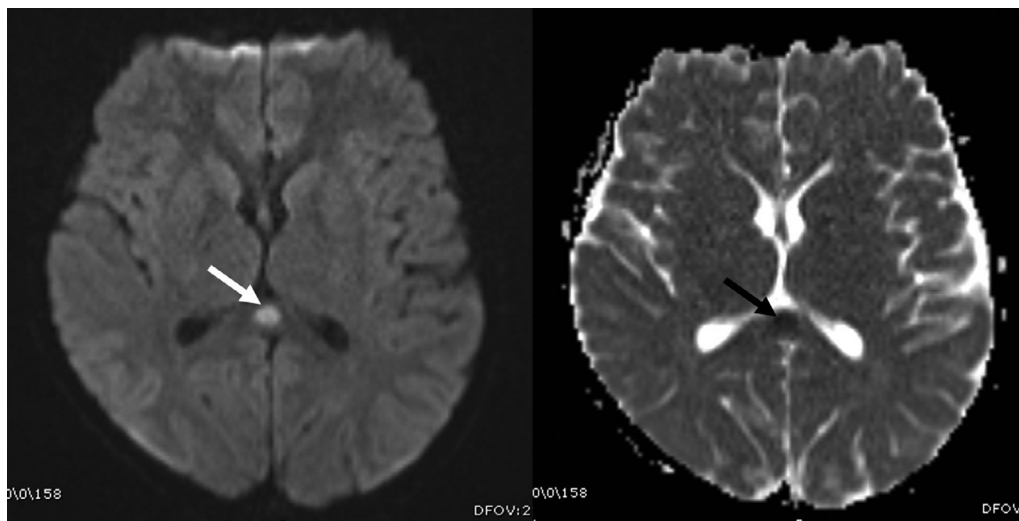


Fig 3. Cranial MRI image of an 10-year-old male showing diffusion restriction in an oval form in the posterior part of the body of the corpus callosum (white arrow) in diffusion-weighted sequences.

hemispheres, periaqueductal region, mesencephalon, bilateral hypothalamic region, bilateral thalamus, lentiform nucleus, caudate nucleus, deep white matter, and subcortical area with no diffusion restriction or contrast enhancement. These entities were considered as ADEM-like lesions (Fig 4a–c). The spinal MRI of the same patient was normal. Following the initiation of treatment, the clinical state of the patient first improved, but five days later, seizures were observed again. Although the lesions had completely disappeared according to the cranial MRI examination, new pathological signal changes were in the bilateral parietooccipital and bilateral frontoparietal regions without contrast enhancement or diffusion restriction. These new lesions were evaluated as posterior

reversible encephalopathy syndrome (PRES; Fig 4d–f). In another patient with seizure complaints, MRI was performed in the bilateral frontoparietal region, and bilateral parietal lesions with cortico–subcortical symmetrical diffusion restriction and contrast enhancement were detected. This patient was evaluated to have an ADEM-like lesion, which was found to increase and be accompanied by necrotic areas in the repeated MRI examination after the aggravation of clinical manifestation during the follow-up. Furthermore, laminar necrosis was added to the findings, and it was evaluated as acute hemorrhagic necrotizing encephalomyelitis (Fig 5). The another patient had presented with the complaint of inability to walk and had complete loss of deep tendon

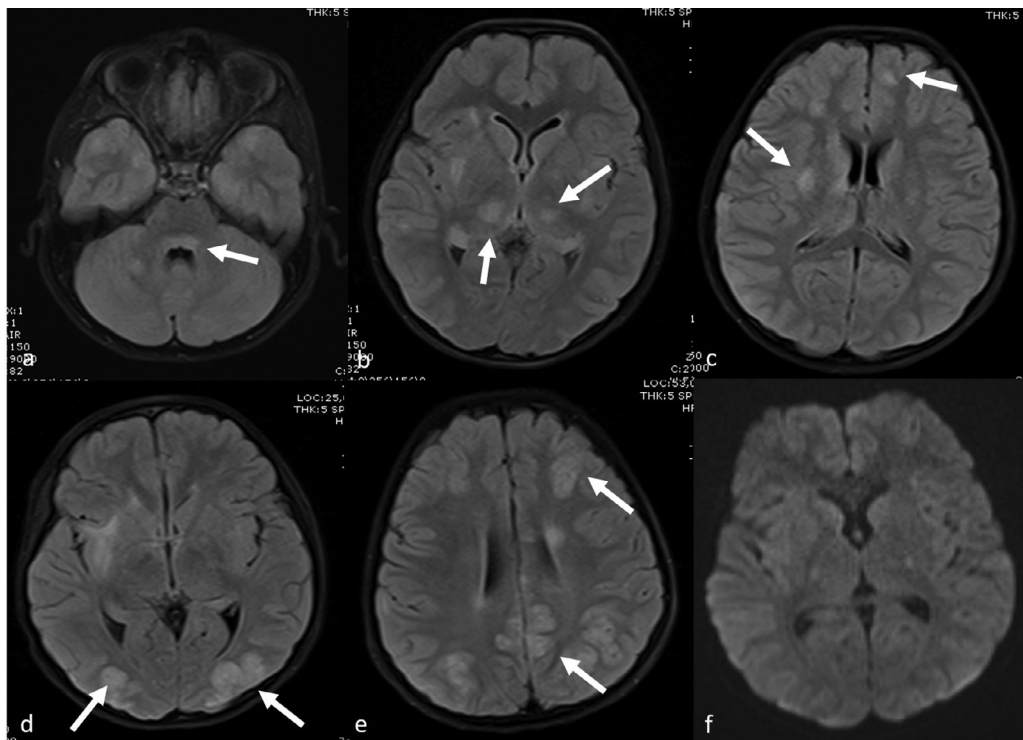


Fig 4. Cranial MRI examination of a nine-year-old male showing ADEM-like signal changes without diffusion restriction (a-c) in the cerebellar hemispheres, periaqueductal region, mesencephalon, bilateral hypothalamic region, bilateral thalamus, lentiform nucleus, caudate nucleus and deep white matter and subcortical area. Cranial MRI performed five days after the seizure recurred indicates that the lesions have completely disappeared, but there are new pathological signal changes in bilateral parietooccipital region and bilateral frontoparietal region, which do not show contrast enhancement or diffusion restriction. These new lesions were evaluated as PRES.

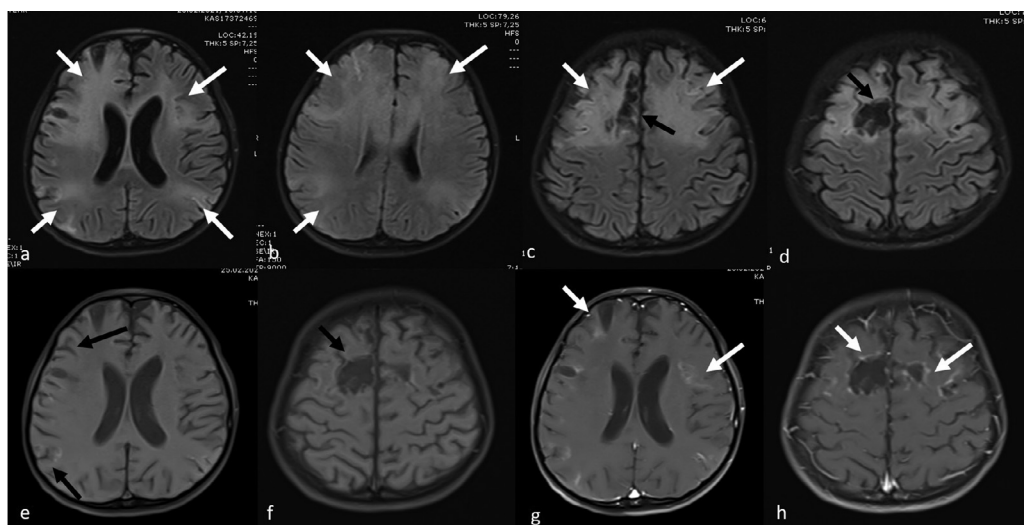


Fig 5. Cranial MRI examination of a nine-year-old male showing ADEM-like pathological signal changes in bilateral symmetrical deep and subcortical white matter (white arrow) (a-d) and necrosis in the parenchyma (black arrow) in the follow-up. The patient also has laminar necrosis (black arrow), and contrast enhancement is seen in the affected areas (white arrow), evaluated as acute hemorrhagic necrotizing encephalomyelitis (e-h).

reflexes when he arrived. While the cranial MRI was normal, the contrast-enhanced spinal MRI revealed diffuse contrast involvement in the cauda equina fibers and nerve roots. When combined with electromyography (EMG) findings, the acute motor axonal neuropathy (AMAN) type was

evaluated as Guillain-Barré syndrome (Fig 6). The another patient presented with disorientation and involvement of various systems. MRI was performed and revealed cerebral and cerebellar atrophy, as well as bilateral symmetrical diffuse signal changes and volume loss in periventricular deep white

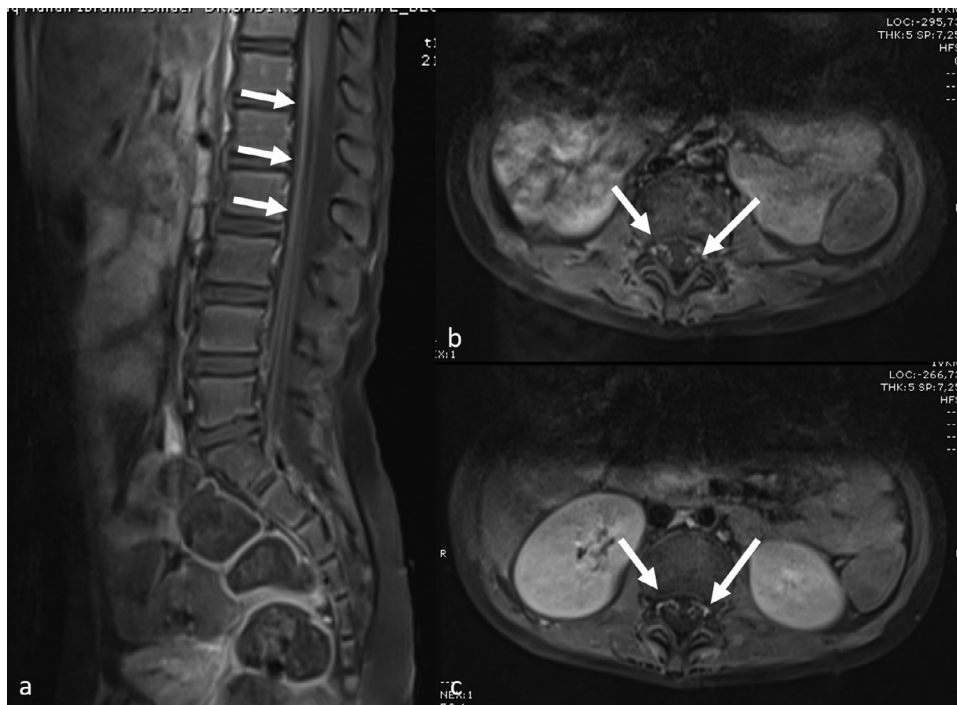


Fig 6. Spinal MRI images of a six-year-old male with muscle weakness diagnosed with Guillain-Barré syndrome based on contrast enhancement in the cauda equina fibers and nerve roots in the sagittal (a) and axial (b, c) planes

matter. The findings were not directly linked to COVID-19. Although there were neurological findings in four cases (%29), no cranial imaging finding was observed.

DISCUSSION

MIS-C can be defined as inflammation caused by excessive immune response that develops after acute COVID-19 infection in children. Unlike acute COVID-19 infection, MIS-C comorbidity does not occur in children but it develops in healthy children (1). Pneumonia and flu-like symptoms observed in acute disease are not present in these children. Clinical findings in children appear within two to three weeks after previous infection. RT-PCR or serology positivity for SARS-CoV-2, indicating that the infection was passed (2). With the increasing number of cases, WHO (3), Royal Collage (4) and disease control unit (5) have defined diagnostic criteria for this newly identified disease.

Imaging findings of MIS-C associated with COVID-19 differ depending on the inflammatory process involved in various systems. A limited number of studies have shown that radiological findings observed are nonspecific and cannot be used as diagnostic criteria. However, some radiological findings can alert the radiologist and clinician to the suspicion of MIS-C. In particular, if there is a history of contact with a COVID-19-infected individual and other possible diagnoses have been excluded, radiological findings can be significant in the diagnosis of MIS-C.

MIS-C cases present with a wide range of clinical symptoms according to the system affected. The most frequently

reported general and gastrointestinal symptoms were fever, rash, conjunctivitis and weakness and vomiting, abdominal pain and diarrhea. Neurological symptoms were seizure, neck stiffness, and inability to walk while respiratory symptoms included cough and respiratory distress. In addition to chest X-ray and echocardiography being routinely performed in every patient admitted to our hospital and considered to have MIS-C, direct abdominal radiography and US are also undertaken in those with abdominal complaints, abdominal CT if necessary, thorax CT in the presence of respiratory complaints, and cranial and spinal MRI for those with neurological complaints if required. In our study, the radiological imaging findings found were consistent with the clinical findings of patients with MIS-C previously reported by Blumfield et al. (6). In our study, some cases presented with the involvement of a single system while others had multisystem involvement and related radiological findings.

Unlike acute infection, lung involvement is rare in MIS-C. Typical lung findings observed in acute COVID-19 infection, such as peripherally located multiple ground glass and consolidation areas are not seen in MIS-C (14–16). The most common findings observed on chest radiography are perihilar prominence and peribronchial thickening, which may be due to airway inflammation (7,8). In our series, lung involvement was detected in only 29% of the cases, while peribronchial thickening and perihilar prominence were the most common findings on chest X-ray. Blumfield et al. (6) frequently reported cardiomegaly and pleural effusion in their series. In our series, consolidation and associated pleural effusion were observed in the lower lobes in five cases, and

diffuse ground glass appearance and consolidation were present in one case. Fenlon et al. (8) suggested that this might be due to cardiogenic or non-cardiogenic edema/acute respiratory distress syndrome due to cardiac dysfunction and multiple organ failure caused by hyperinflammation or it might be a result of MIS-C accompanying acute COVID-19 infection or other infectious and non-infectious causes. Pulmonary embolism did not develop in any of our patients with pulmonary involvement.

The most common finding observed in MIS-C is acute myocardial dysfunction. Left ventricular systolic dysfunction and decreased ejection fractions are reported in the literature. In addition, coronary artery dilatation and aneurysm and pericarditis have been reported (11–13). Echocardiography is usually sufficient for the diagnosis. In the echocardiography of our cases, we observed that myocardium was affected in 14 (31%). In all cases, there was a decrease in left ventricular systolic function and varying degrees of ejection fraction. The use of cardiac MRI for the diagnosis of myocarditis in MIS-C cases has been previously reported. Diffuse edema findings in the myocardial muscle are observed in cardiac MRI (14). MRI findings suggestive of fibrosis and necrosis were not detected in our cases. We performed cardiac MRI in one of our patients with multisystem involvement, but the findings were the same as echocardiography findings.

Abdominal complaints were the most common in our cases; therefore, abdominal imaging was performed. In these cases, the most common findings were edema and wall thickening around the gallbladder, multiple mesenteric lymph nodes over 5 mm in the short axis in the right lower quadrant, thickening of the ileal intestinal walls, and free fluid, which is in agreement with other studies (6–8). Since the findings in five cases suggested acute appendicitis, abdominal US and then CT examinations were also performed. The appendix was evaluated to be normal in these examinations. Hameed (7), Fenlon (8), and Tullie (9) et al. reported that such cases can most often be confused with acute appendicitis and cause unnecessary operations. There are many lymph nodes in the right lower quadrant of the abdomen, and the ileal loops contain Peyer's patches with lymphoid tissue. Similar to mesenteric lymphadenitis, inflammation in lymphatic structures causes symptoms similar to acute appendicitis. These abdominal findings observed in MIS-C cases have been attributed to systemic inflammation, hypoalbuminemia, serositis, fluid overload, and cardiac failure. In a case series of Hameed et al., solid organ infarctions such as splenic infarction have been reported and associated with the inflammatory vasculitis of vascular structures that feed the organs (7). A thrombus is frequently observed in various abdominal large vascular structures due to the increase in coagulation factors in adult COVID-19 cases. In addition, the liver and the biliary system are the most frequently affected systems after pulmonary involvement (10). There are no similar radiological findings reported in the acute period in children. The most common findings in our study were hepatomegaly and hepatosplenomegaly. In addition, in eight cases in our study,

although there was an increase in pancreatic and hepatic enzymes, no remarkable radiological finding was detected. Radiological findings showing pancreatic and liver involvement were observed in one patient. In one of our patients, a thrombus was detected in the vena cava inferior, which we considered to be due to coagulation disorder, while pancreatic involvement and related atrophy and necrosis were detected in the pancreas of another case. In addition, the latter had cholestasis in the intrahepatic biliary tracts due to liver involvement, which we visualized radiologically. Although the etiology of similar lesions in adults is not clearly explained, it has been linked to the direct damage of cells, inflammatory process, or hepatotoxic effect of drugs (10). We consider that these findings may be due to vasculitis caused by inflammation in pediatric cases.

Although we conducted the study in a single center, we had a higher number of cases with neurological and neuroradiological findings compared to previous case series. In adult cases, infection due to COVID-19, venous sinus thrombus, encephalomyelitis, Guillain-Barré syndrome, Miller Fisher syndrome, myelitis, and PRES have been described in the literature (17,18). The neurological findings of COVID 19 and MIS-C in children have been attributed to direct neuronal damage, vascular endothelial damage, and inflammatory and autoimmune damage (19). The neuroradiological findings reported in MIS-C cases in the literature are from a multicenter study (20) and case reports (21–23) and remain limited. Orman et al. found neuroradiological findings in only 10% of the cases diagnosed with COVID-19 who underwent a neuroradiological examination (24). These findings were reported as PRES and hippocampal signal changes. Different neurological findings were observed in 31% of our MIS-C cases, and we observed radiological findings in 64% of these patients. While only two of our cases had other system involvement, the others presented with only neurological findings. The most common finding was RESLES, which is also frequently reported in the literature. The most common cause of transient splenic lesions in children is mild encephalopathy with a reversible splenic lesion (MERS), which develops secondary to focal intramyelinic edema due to inflammation (21). In addition, RESLES may develop due to ischemia, status epilepticus, and electrolyte irregularities. The splenic lesion is observed in the posterior part of the corpus callosum body as an oval form of temporary diffusion restriction. In our series, it was observed in 43% of the cases and disappeared in the control diffusion MRI examinations performed after the initiation of treatment and improvement of neurological findings. Furthermore, one of our cases presented with ADEM-like lesions, while another case developed acute hemorrhagic necrotizing encephalomyelitis. A patient with gait disorder and muscle weakness was diagnosed with Guillain-Barré syndrome. In a retrospective study conducted by Lindan et al., ADEM-like lesions were the most frequent findings, while myelitis and enhancement were also observed in cranial nerve and spinal nerve roots. ADEM-like lesions are in the form of large and patchy lesions that swallow

white and gray matter and can show the limitation of contrast and diffusion (20). Similar findings to our case have been reported in adults and patients with acute hemorrhagic necrotizing encephalomyelitis, which is rarely described on a case-by-case basis in the literature (17,18,25). Guillain-Barré syndrome is another pathology reported in MIS-C cases (26). We did not observe myelitis in our cases, in contrast to Kaur et al. (27). It is considered that all the findings observed in MIS-C cases are primarily due to parainfectious inflammation due to the immune response involving the brain, spinal cord, cranial nerve, and nerve roots (20).

The limitations of our study include the single-center and retrospective design of the study and the small number of cases. Although the number of MIS-C cases is increasing, radiological imaging findings that can be demonstrated remain limited. As the number of cases is reported from different centers, our knowledge in this area will further increase; therefore, there is a need for multicenter multidisciplinary studies.

The radiological findings seen in MIS-C associated with COVID-19 in pediatric cases are correlated with the affected system. According to the system involved, there is no specific finding for the disease. Radiological imaging is not the primary method for diagnosis. The focus of imaging should be to exclude other processes and complications that affect patient management. However, radiologists should be knowledgeable about possible findings that can be observed in MIS-C associated with COVID-19 and conduct further investigations in case of suspicion.

REFERENCES

- Biko D, Ramirez-Suarez K, Barrera C, et al. Imaging of children with COVID-19: experience from a tertiary children's hospital in the United States. *Pediatr Radiol* 2021; 51(2):239-247. doi:10.1007/s00247-020-04830-x. Epub 2020 Sep 18.
- Jiang L, Tang K, Lvin M, et al. COVID-19 and multisystem inflammatory syndrome in children and adolescents. *Lancet Infect Dis* 2020; 20(11):e276-e288. doi:10.1016/S1473-3099(20)30651-4. Epub 2020 Aug 17.
- World Health Organization Multisystem inflammatory syndrome in children and adolescents with COVID-19. Published May 15, 2020. <https://www.who.int/publication/i/item/>
- Royal Collage of Pediatrics and child health: Guidance pediatric multisystem inflammatory syndrome temporally associated with COVID-19. Accessed May 22, 2020. Update September 2020. <https://rcph.ac.uk/resources/guidance-paediatric-multisystem-inflammatory-syndrome-temporally-associated-covid-19>.
- Centers for disease control and prevention emergency preparedness and response: health alert network. Published May 14, 2020. <https://www.emergency.cdc.gov/han/index.asp>
- Blumfield E, Levin T, Kurian J, et al. Imaging findings in multisystem inflammatory syndrome in children (MIS-C) associated with coronavirus disease (COVID-19). *AJR Am J Roentgenol* 2021; 216(2):507-517.
- Hameed S, Elbaaly H, Reid C, et al. Spectrum of imaging findings at chest radiography, US, CT and MRI in multisystem inflammatory syndrome in children associated with COVID-19. *Radiology* 2021; 298(1):E1-E10. doi:10.1148/radiol.202020543. Epub 2020 Jun 25.
- Fenlon E, Chen S, Ruzal-Shapiro C, et al. Extracardiac imaging findings in COVID-19 associated multisystem inflammatory syndrome in children. *Pediatr Radiol* 2021; 1-9. doi:10.1007/s00247-020-04929-1.
- Tullie L, Ford K, Bisharat M, et al. Gastrointestinal features in children with COVID-19: an observation of varied presentation in eight children. *Lancet Child Adolesc Health* 2020; 4(7):e19-e20.
- Revzin M, Raza S, Srivastava N, et al. Multisystem imaging manifestations of COVID-19, Part 2: From cardiac complications to pediatric manifestations. *Radiographics* 2020; 40(7):1866-1892. doi:10.1148/rg.2020200195.
- Sperotto F, Friedman K, Son M, et al. Cardiac manifestations in SARS-CoV-2 associated multisystem inflammatory syndrome in children: a comprehensive review and proposed clinical approach. *Eur J Pediatr* 2021; 180(2):307-322. doi:10.1007/s00431-020-03766-6.
- Alsaied T, Tremoulet AH Burns J, et al. Review of cardiac involvement in multisystem inflammatory syndrome in children. *Circulation* 2021; 143(1):78-88. doi:10.1161/CIRCULATIONAHA.120.049836.
- Blondiaux E, Parisot P, Redhail A, et al. Cardiac MRI of children with multisystem inflammatory syndrome (MIS-C) associated with COVID-19. *Radiology* 2020; 297(3):E283-E288. doi:10.1148/radiol.2020202288.
- Palabiyik F, Kokurcan S, Hatipoglu N, et al. Imaging of COVID-19 pneumonia in children. *Br J Radiol* 2020; 93(1113):20200647doi:10.1259/bjr.20200647. Epub 2020 Jul 30.
- Bayramoglu Z, Canipek E, Comert R, et al. Imaging features of pediatric COVID-19 on chest radiography and chest CT: A retrospective, single center study. *Acad Radiol* 2021; 28(1):18-27. doi:10.1016/j.acra.2020.10.002. Epub 2020 Oct 5.
- Katal S, Johnston S, Johnston J, et al. Imaging Findings of SARS-CoV-2 Infection in Pediatrics: A Systematic Review of Coronavirus Disease 2019 (COVID-19) in 850 Patients. *Acad Radiol*. 27(11):1608-1621
- Harapan B, Yoo H. Neurological symptoms, manifestations and complications associated with severe acute respiratory syndrome coronavirus 2 (SARS-CoV-2) and coronavirus disease 19 (COVID-19). *J Neurol* 2021; 1-13. doi:10.1007/s00415-021-10406-y.
- Kremer S, Lersy K, de Seze J, et al. Brain MRI findings in severe COVID-19: A retrospective observational study. *Radiology* 2020; 297(2):E242-E251. doi:10.1148/radiol.2020202222. Epub 2020 Jun 16.
- Lin J, Asfour A, Sewell T, et al. Neurological issues in children with COVID-19. *Neurosci Lett*. 2021; 743:135567doi:10.1016/j.neulet.2020.135567.
- Lindan C, Mankad K, Ram D et al. Neuroimaging manifestations in children with SARS-CoV-2 infection: a multinational, multicentre collaborative study. *Lancet Child Adolesc Health*. 2021;5(3):167-177. doi:10.1016/S2352-4642(20)30362-X. Epub 2020 Dec 16.
- Abdul-Mannan O, Eyre M, Lobel U, et al. Neurologic and radiographic findings associated with COVID-19 infection in children. *JAMA Neurol* 2020; 77(11):1-6. doi:10.1001/jamaneurol.2020.2687.
- Bektas G, Akcay N, Boydag K, et al. Reversible splenic lesion syndrome associated with SARS-Cov-2 infection in two children. *Brain Dev* 2021; 43(2):230-233. doi:10.1016/j.braindev.2020.10.002. Epub 2020 Oct 13.
- Gaur P, Dixon L, Jones B, et al. COVID-19-associated cytotoxic lesions of the corpus callosum. *AJNR Am J Neuroradiol* 2020; 41(10):1905-1907. doi:10.3174/ajnr.A6713. Epub 2020 Aug 20.
- Orman G, Desai N, Kralik S, et al. Neuroimaging offers low yield in children positive for SARS-CoV-2. *AJNR Am J Neuroradiol* 2021. doi:10.3174/ajnr.A7022.
- Poyiadji N, Shahin G, Noujaim D, et al. COVID-19 associated acute hemorrhagic necrotizing encephalopathy: Imaging features. *Radiology* 2020; 296(2):E119-E120. doi:10.1148/radiol.2020201187.
- Khalifa M, Zakaria F, Ragab Y, et al. Guillian-Barre syndrome associated with SARS-CoV-2 detection and a COVID-19 infection in a child. *J Pediatric Infect Dis Soc* 2020; 9(4):510-513. doi:10.1093/jpids/piaa086.
- Kaur H, Mason A, Bajracharya M, et al. Transverse myelitis in child with COVID-19. *Pediatr Neurol* 2020; 112:5-6. doi:10.1016/j.pediatrneurol.2020.07.017. Epub 2020 Jul 29.